

# Generalizing Scaling Laws for Dense and Sparse Large Language Models

Md Arafat Hossain

Department of Computer Science  
Iowa State University

Email: arafat@iastate.edu

Xingfu Wu, Valerie Taylor

Mathematics and Computer Science Division  
Argonne National Laboratory

Email: {xingfu.wu, vtaylor}@anl.gov

Ali Jannesari

Department of Computer Science  
Iowa State University

Email: jannesar@iastate.edu

**Abstract**—Despite recent advancements of large language models (LLMs), optimally predicting the model size for LLM pretraining or allocating optimal resources still remains a challenge. Several efforts have addressed the challenge by proposing different empirical scaling laws, but almost all of them are architecture-specific (dense or sparse). In this work we revisit existing empirical scaling laws and propose a generalized scaling law to provide a unified framework that is applicable to both dense and sparse large language models. We evaluate and compare our proposed scaling law with existing scaling laws and demonstrate that our proposed scaling law captures the scaling behavior of existing scaling laws. Further, we show an IsoFLOP comparison between our proposed scaling law and the state-of-the-art scaling law to illustrate the effectiveness of our proposed scaling law for Mixture-of-Expert (MoE)-based very large LLMs like DeepSeek-V3. Our proposed scaling law can be used to estimate the best model hyperparameters (Model size, Tokens and Compute) for a given sparsity or to identify the optimal sparsity for the given model hyperparameters.

**Index Terms**—LLMs, Dense models, Sparse models, Scaling laws, Sparsity

## I. INTRODUCTION

In recent years, transformer architectures [1] have revolutionized the deep learning approach especially the field of natural language processing with the development of transformer-based architectures [1] such as BERT [2] and GPT-3 [3] etc. Transformer architecture is now the foundation for the majority of popular large language models (LLMs). Since the release of ChatGPT LLMs have gained more attention across diverse domains as a key innovative technology. With the growing popularity across diverse domain there is an increasing need to scale LLM knowledge and accuracy while also reducing the inference latency and training cost. However, achieving these goals is fundamentally challenging due to the computational structure of standard transformer models, as computation grows rapidly with the increase of model size and context length.

In traditional transformer architecture, parameters in every layer are activated to process every token. Each token passes through the same feed-forward network, and in a multi-head attention setting, every attention considers every other position. These traditional forms of transformers are called dense transformers. The complex and exhaustive architecture allows the dense models to understand the rich contextual meaning of the input dataset, but it comes with a high computational cost that scales with both model size and sequence length.

One way to reduce the cost is to introduce sparsity where all the available parameters are not used to process a token in a sparse model. There are several ways to introduce sparsity, but in this work we focus on two methods: pruning [4] and mixture of

experts (MoE) [5]. Pruning-based sparsity permanently removes parameters from the model. Pruning can be categorized into three main groups [4] namely: structured pruning, unstructured pruning, and semi-structured pruning. In structured pruning, entire higher-level units or even whole layers are removed; this process delivers universal speedup but sometimes at the cost of accuracy. In unstructured pruning, individual weights are removed from anywhere in the network; usually the least important weights are pruned. In semi-structured pruning, one tries to strike a balance between unstructured and structured pruning approaches by enforcing fixed pruning patterns in small regions of the network. On the other hand, in MoE-based models the feed-forward network for a transformer model is replicated multiple times, and each of these copies is called an “expert”. In the MoE-based models only a fraction of experts are activated per token, instead of all the experts and that’s how sparsity is introduced. The number of activated experts is a fixed value and determines the sparsity level. The tokens are routed to different experts during the pretraining process. The size of the experts is usually equal to the size of the feed-forward network but can differ too.

Several models [6]–[10] have been developed over the past few years with traditional dense architecture. But lately, sparse transformers [11]—have become extremely popular, and several models [12]–[19] have been developed using the concept of sparsification. One common factor among all these models is that as they are evolving, their size has been increasing significantly from GPT-2 with 1.5 billion parameters [20] to PaLM with 540 billion parameters [9], to DeepSeek-V3, a strong mixture-of-experts (MoE) language model with 671 billion parameters, 37 billion of which are activated for each token [21], which has 94.49% sparsity. The reason is, it has been proven that as model size, dataset size, and the amount of compute used for training increase, LLM performance improves smoothly [22]. However with the increase of size, these models require large training datasets, eventually increasing the compute budget [22], [23] to several petaFLOP/s-days of computation to achieve optimal performance. This makes LLM training time-consuming and resource intensive. As a result, determining the optimal allocation of resources, model size, and training data and estimating the training performance before conducting the actual training is crucial.

Scaling laws are the empirical relationships, often expressed as power laws—describe a model’s performance based on allocated resources. These laws help determine the optimal model size and data volume for a given compute budget to achieve

optimal pretraining performance. Several empirical scaling laws based on different LLM architectures have been proposed in recent years [22]–[29]. Few scaling law works focused on training precision [30], distillation [31], and quantization [32]. Several studies have also been done on vision [24], audio [33], [34], and mixed-modal language models [35]. This interest in scaling laws for different domains makes them pivotal in deep neural network research. However, until now, nearly all existing approaches have been architecture-specific (dense or sparse) and also use different scaling law coefficients (details in Section II) which makes it difficult to perform cross-architecture comparisons and budget planning. In this work we show that transformers, regardless of dense and sparse architectures, exhibit a common scaling behavior which depends on the number of active/nonzero parameters. To demonstrate that, we generalize the existing empirical scaling laws to propose a scaling law that enables accurate performance predictions and optimal resource allocation across architectures. In this paper we focus on the scaling laws for both dense and sparse LLMs. We make the following contributions:

- We discuss the existing empirical scaling laws for dense and sparse LLMs and their limitations (Section II).
- We propose a generalized scaling law for both dense and sparse LLMs and discuss the relationship between the proposed scaling law and the existing laws (Section III).
- We evaluate and compare the performance of the proposed scaling law and the existing laws using some test models to demonstrate its effectiveness, and we present hyperparameter optimization results for some existing scaling laws (Section IV).

Section V summarizes this work and suggests avenues for potential future research.

## II. SCALING LAWS FOR LLMs

Based on the number of parameters available in the architecture and the number of parameters that are being used during pretraining, transformer models can be categorized into dense and sparse transformers. Previous works [6]–[10], [12]–[19] have shown that these models exhibit different behavior during pretraining as they scale, and hence their scaling behaviors are studied separately.

### A. Scaling Laws for Dense Models

Traditional transformer models are dense in nature. Kaplan et al. [22] studied the behavior of dense LLMs with a series of experiments by monitoring different hyperparameters: model size, model shape, total compute, data volume, and batch size during pretraining. The authors established that model loss depends strongly on scale, which consists of the number of model parameters  $N$ , the dataset size (number of tokens)  $D$ , and the amount of compute  $C$  used for training. It also depends mildly on other architectural hyperparameters such as model shape: depth and width. For dense models, the compute  $C$  (training FLOPs) required to train a transformer model with  $N$  parameters and  $D$  tokens is  $C = 6ND$  [22] because approximately 6 floating point operations are needed for every parameter in the model and every training sample. The authors also suggested that if compute is increased by 10 times, then model size should be increased by 5.5 times and dataset size by

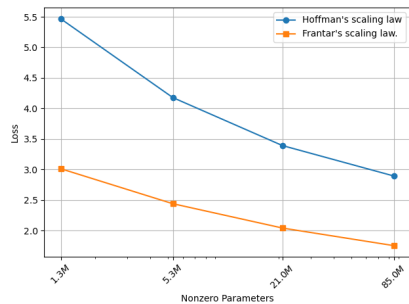


Fig. 1: Comparison between Hoffman scaling law and Frantar scaling law at 0% sparsity.

1.8 times to avoid overfitting. They represented training loss as a function of number of parameters and data size and proposed the empirical scaling law:

$$L(N, D) = \left[ \left( \frac{N_C}{N} \right)^{\frac{\alpha_N}{\alpha_D}} + \frac{D_C}{D} \right]^{\alpha_D} \quad (1)$$

The best-fitted values for the coefficients and exponents in Equation 1 are listed in Table I.

Coefficients	$\alpha_N$	$\alpha_D$	$N_C$	$D_C$
Values	0.076	0.103	$6.4 \times 10^{13}$	$1.8 \times 10^{13}$

TABLE I: Fitted parameter values for Equation 1

Using three different approaches—fixed model size with varying numbers of training tokens, IsoFLOP profiling, and parametric function fitting—Hoffmann et al. [23] extended and corrected Equation 1 in [22] and concluded that model size and number of tokens should be increased in proportion to avoid overfitting. The authors represented training loss as a combination of irreducible loss or entropy  $e$ , a parameter-dependent term or the loss incurred by a model of fixed parameter size, and a data size term or the loss induced by a fixed number of training steps. Based on the observations from their three experiments, the authors proposed Equation 2 as their scaling law.

$$L(N, D) = e + \frac{a}{N^\alpha} + \frac{b}{D^\beta} \quad (2)$$

This law establishes a power-law relationship between loss  $L$ ,  $N$ , and  $D$ . Here  $e$  captures the entropy of the natural text, which is the minimum loss as both  $N$  and  $D$  approach infinity. The second term (parameter-dependent term) captures the inverse relationship between  $N$  and loss. The third term (data-dependent term) captures the impact of  $D$  on loss. The constants  $a$  and  $b$  and the exponents  $\alpha$  and  $\beta$  are determined empirically through some experiments and fitting the data. Its best-fitted values for the coefficients and exponents are listed in Table II. Equation 2 currently is the state-of-the-art empirical scaling law for dense LLMs. For the rest of the paper, we will refer Equation 2 as Hoffman scaling law.

Coefficients	$e$	$a$	$b$	$\alpha$	$\beta$
Values	1.69	406.4	410.7	0.34	0.28

TABLE II: Fitted parameter values for Equation 2

## B. Scaling Laws for Sparse Models

Sparse LLMs use only a subset of the parameters available in the models. Several works had proposed scaling laws for sparse transformer models [24], [25], [28]. These scaling laws are based on different sparsification methods. In this work we focus on two types of sparsifications: pruning and mixture-of-experts (MoE).

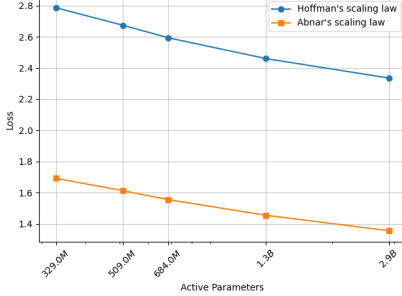


Fig. 2: Comparison between Hoffman scaling law and Abnar scaling law at 0% sparsity.

1) *Pruned Models*: One way to introduce sparsity in transformer models is pruning, where a subset of parameters are removed or masked and are not used during the forward pass or backpropagation, hence making no contribution to the training process. Frantar et al. [24] studied the scaling behavior of models pruned by unstructured pruning. In their work, the authors defined sparsity,  $S = \frac{\text{Total Parameters} - \text{Nonzero Parameters}}{\text{Total Parameters}}$ . Based on the pretraining results of 48 models with different sparsity levels, numbers of nonzero parameters and training tokens, the authors claimed that sparsity introduced by pruning affects only the parameter-dependent term of Hoffman scaling law and has minor to no impact on the data-dependent term. The authors also claim that increasing sparsity leads to a better pretraining loss. Their experimental results also showed that as the number of nonzero parameters and training tokens—in other words, total compute increased the pretraining loss keeps getting better, which holds the claim of Hoffman scaling law [23]. Using the Hoffman scaling law as the foundation, the authors fitted loss as a function of nonzero parameters  $N$ , data  $D$ , and sparsity  $S$  as shown in Equation 3.

$$L(N, D, S) = (a_S(1 - S)^{b_S} + c_S) \cdot \left(\frac{1}{N}\right)^{b_N} + \left(\frac{a_D}{D}\right)^{b_D} + c \quad (3)$$

Following the similar approach of [23] the authors presented the best-fitted values for the scaling law coefficients of Equation 3. Table III lists the scaling law parameter values mentioned in [24]. For the rest of the paper, we will refer to Equation 3 as the Frantar scaling law.

Coefficients	$a_S$	$b_S$	$c_S$	$b_N$	$a_D$	$b_D$	$c$
Values	16.8	0.722	45	0.245	$6.90 \times 10^8$	0.203	0.651

TABLE III: Fitted parameter values for Equation 3

To draw the similarities between Hoffman scaling law in Equation 2 and Frantar scaling law in Equation 3, we used the similar symbols used in Hoffman scaling law to reformat the scaling law coefficients in Frantar scaling law. We used  $e$  instead

of  $c$  to capture the lower bound on the loss that represents the inherent stochasticity of the modeling problem. We replaced  $b_N$  and  $b_D$  with  $\alpha$  and  $\beta$ , respectively, and  $a_D^{b_D}$  with  $b$ .  $c_S$  is the constant sparsity factor. The reformatted version of Frantar scaling law is Equation 4.

$$L(N, D, S) = e + (a_S(1 - S)^{b_S} + c_S) \frac{1}{N^\alpha} + \frac{b}{D^\beta} \quad (4)$$

Equation 4 helps visualize the transition from the dense Hoffman scaling law Equation 2 to the sparse Frantar scaling law Equation 3 in order to investigate which factor is directly impacted by sparsity. Based on the changes in representation, we recalculate the best-fitted values for the scaling law coefficients in the reformatted Frantar scaling law, and the values are listed in Table IV.

Coefficients	$a_S$	$b_S$	$c_S$	$b$	$\alpha$	$\beta$	$e$
Values	16.8	0.722	45	62.271	0.245	0.203	0.651

TABLE IV: Fitted parameter values for Equation 4

While Equation 4 functionally captures the effect of sparsity on loss, the maximum sparsity used in the experiments was 87.5% [24] while other works [25] show that better performance gain can be achieved by introducing even more sparsity (even at 98% sparsity). The largest model used in Frantar scaling law experiments had only 85M nonzero parameters which are relatively much smaller. Although this work used the Hoffman scaling law as baseline, at 0% sparsity or for dense models with the same dataset, Equation 4 provides different loss predictions than those in Hoffman scaling law with an average MSE (Mean Squared Error) of 3.04, as shown in Figure 1. Thus, we can conclude that Hoffman scaling law is not a special case of Frantar scaling law where sparsity is 0%

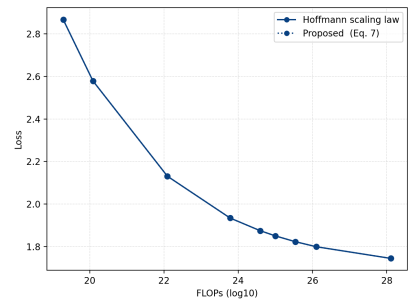


Fig. 3: Loss prediction of Hoffman scaling law and the proposed scaling law.

2) *MoE Models*: Another way to introduce sparsity is to use the mixture-of-experts (MoE) method [5] where the feed-forward network of a transformer model is replicated multiple times and each of these copies is called an “expert.” Only a fraction of experts are activated per token. The tokens are routed to different experts during the pretraining process.

Abnar et al. [25] investigated the sparse MoEs through a large-scale empirical study. The authors defined sparsity,  $S = \frac{E-K}{E}$ , where  $E$  is the total number of experts and  $K$  is the number of active experts. For five ( $3e19$ ,  $6e19$ ,  $1e20$ ,  $3e20$ , and  $1e21$ ) different compute budgets and seven (0%, 25%, 50%, 75%, 90%, 95%, and 98%) different

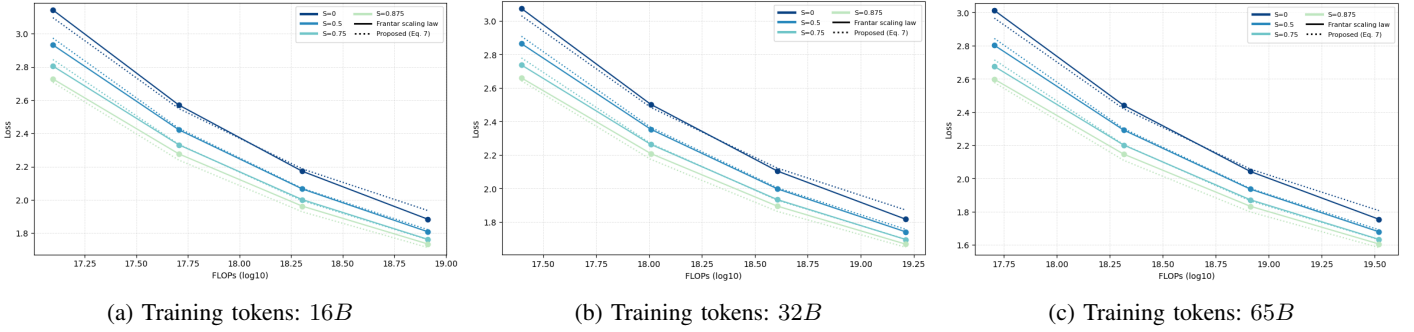


Fig. 4: As sparsity and the number of nonzero/active parameters increase, the pretraining loss decreases. In each figure, the number of non-zero parameters in the models used ranged from  $1.3M - 85M$  with varying sparsity levels, and the number of training tokens is mentioned in the subcaption.

sparsities, different models were trained. The conclusion they made was that as we increase sparsity along with model size and number of training tokens, the pretraining loss decreases. For IsoFLOP experiments, they noticed that each for a specific sparsity level, each model size has a sweet spot. Until that spot, the pretraining loss keeps decreasing, and beyond that spot, pretraining loss keeps increasing. Based on the experimental results, the authors proposed Equation 5 as their scaling law. For the rest of the paper, we will refer to Equation 5 as Abnar scaling law.

$$L(N, D, S) = e + \frac{a}{N^\alpha} + \frac{b}{D^\beta} + \frac{c}{(1-S)^\lambda} + \frac{d}{(1-S)^\delta N^\gamma} \quad (5)$$

Through a grid initialization, for a sparsity of 98%, the best-fitted coefficient values in Equation 5 are determined empirically through the experiments and fitting the data shown in Table V.

Coefficients	$e$	$a$	$b$	$c$	$d$
Values	0.94	16612.50	5455.67	0.4598	17.26
Coefficients	$\alpha$	$\beta$	$\lambda$	$\delta$	$\gamma$
Values	0.5962	0.3954	-0.1666	0.1603	0.1595

TABLE V: Fitted parameter values for Equation 5

Abnar scaling law introduced two different terms in the scaling law along with the previous three terms from Equation 2 [23] to capture the impact of sparsity. The newly introduced terms are interdependent. The fifth term  $\frac{d}{(1-S)^\delta N^\gamma}$  in Equation 5 can be interpreted as an active parameter term because the denominator term is a multiplication of  $N$  and  $1-S$ . As the total number of parameters already includes the active parameters, having two different terms for total parameters and active parameters in Equation 5 can be deemed as redundant. While this may help the Abnar scaling law to fit the experimental results better, we later show that this can be represented in a generalized way without introducing redundancy.

Abnar scaling law also used Hoffman scaling law as the base. We compared both of these laws at 0% sparsity using the same model size and data size used in Abnar scaling law experiments. The results were off from each other with an average MSE of 1.06 in Figure 2.

### III. GENERALIZING SCALING LAWS

We observed that regardless of the dense or sparse architecture, all the previous works mentioned so far use the

number of nonzero or active parameters to measure the total compute. Hoffman et al. [23] used  $C = 6ND$  where  $N$  is the total number of parameters and for dense models this is the number of nonzero/active parameters. Abnar et al. [25] used  $C = 6N_a D$  where  $N_a$  is the number of active parameters. Frantar et al. [24] used  $C = 6ND \cdot c_{mul}(S)$  where the authors used dense Hoffman’s compute formula and multiplied it by a sparsity-dependent factor  $c_{mul}(S)$ . We have also observed in the preceding section that the mentioned sparse scaling laws had their limitations and do not replicate the dense scaling law behavior when the sparsity is 0%. In Section I we have also discussed that due to the architecture-specific nature of existing scaling laws where some scaling laws take total parameters into account for their scaling law and some use the number of nonzero/active parameters, cross-architecture comparison and budget planning become challenging. On top of that, different scaling laws use different scaling law coefficients that need to be tuned carefully to fit the early experimental results for better prediction. We think that the scaling behavior, regardless of the architecture (dense or sparse), is dependent on the number of active/non-zero parameters and propose a generalized scaling law that can address the earlier-mentioned issues.

This proposed scaling law should 1) be able to describe the scaling behavior for both dense and sparse models; 2) achieve similar predictions and capture the scaling behavior observed in the experiments of [22]–[25] as increasing model size, data size, and compute; and 3) capture the behavior for sparse models as observed in [24], [25] for increasing the sparsity. Furthermore, for 0% sparsity or dense models, the scaling law should behave exactly as the Hoffman scaling law.

For simplicity, we use the term “active parameters” ( $N$ ) for active/nonzero parameters in the MoE and pruned models. For the dense models, the total number of active parameters is the total number of parameters. We use Hoffman scaling law (Equation 2) as the base to propose a generalized scaling law. We define the sparsity as follows:

$$S = \frac{\text{Total Parameters} - \text{Active Parameters}}{\text{Total Parameters}} \quad (6)$$

Where  $0 \leq S < 1$  (The number of active parameters in a model cannot be zero and hence,  $S \neq 1$ ).  $\frac{N}{1-S}$  is the total number of parameters. In the parameter-dependent second term of Hoffman scaling law in Equation 2, we replace  $N$  with  $\frac{N}{1-S}$ ; the parameter-dependent term thus becomes  $\left(\frac{a}{\frac{N}{1-S}}\right)^\alpha$ ,

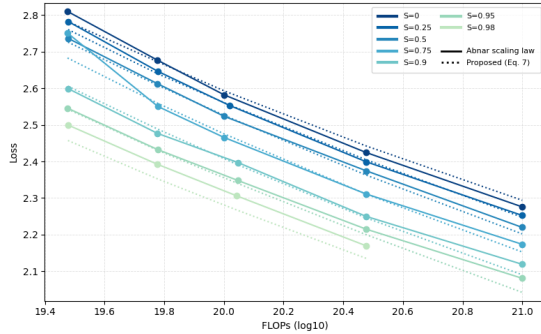


Fig. 5: Scaling behavior and prediction comparison between Abnar scaling law and our proposed scaling law.

which is simplified as  $\frac{a(1-S)^\alpha}{N^\alpha}$ . Similar to the Frantar et al. approach in [24] we introduce an upper-bound constant sparsity factor  $c$ ; but unlike Frantar scaling law, this factor depends on the sparsity  $S$ . So we define the parameter-dependent term as  $(a(1-S)^\alpha + c \cdot S) \frac{1}{N^\alpha}$ .

While  $e$  corresponds to irreducible loss, empirical fits over  $N$  and  $D$  treat the constant as an effective offset. For sparse models, this offset can vary systematically with sparsity. We model this dependence with minimal multiplicative factor  $(1-S)^\gamma$ , preserving the dense limit and power law behavior of scaling laws. Accumulating these changes, we propose Equation 7 as our proposed scaling law.

$$L(N, D, S) = e(1-S)^\gamma + (a(1-S)^\alpha + c \cdot S) \frac{1}{N^\alpha} + \frac{b}{D^\beta} \quad (7)$$

This equation quantifies the impact of sparsity on loss. Notice that we did not change the values of the data-dependent term ( $\frac{b}{D^\beta}$ ) in Equation 2 (Hoffman scaling law), because the work in [24], [25] has shown experimentally that sparsity has no effect on this term.

**Lemma:** If sparsity  $S$  is 0, Equation 7 is the Hoffman scaling law in Equation 2.

If the sparsity  $S$  is 0, the total number of parameters is equal to the total number of active parameters. From Equation 7 we have

$$L(N, D, 0) = e(1-0)^\gamma + (a(1-0)^\alpha + c \cdot 0) \frac{1}{N^\alpha} + \frac{b}{D^\beta} \quad (8)$$

Then, simplifying Equation 8, we have

$$L(N, D, 0) = e + \frac{a}{N^\alpha} + \frac{b}{D^\beta}.$$

From Equation 2, we have

$$L(N, D) = e + \frac{a}{N^\alpha} + \frac{b}{D^\beta}.$$

Because the coefficients  $e, a, b, \alpha, \beta$  are the same, we have  $L(N, D, 0) - L(N, D) = 0$ .

## IV. PERFORMANCE RESULTS AND DISCUSSION

### A. Performance Results

In this section we compare the performance of our proposed scaling law and the previous architecture specific scaling laws for dense and sparse models. We have collected the experimental datasets (number of parameters, number of tokens, and sparsity) used in [23]–[25] shown in Table VI. Hoffman et al. [23]

provided a list of nine models with number of parameters and training tokens used in their experiments. Frantar et al. [24] provided four different numbers of nonzero parameters, three different numbers of training tokens, and four different sparsity levels with a total of 48 experimental runs to collect their experimental results. Abnar et al. [25] used five different numbers of compute budgets, seven different sparsity levels, and a range of model sizes. Then we use these experimental datasets to generate plots for their respective scaling laws and use the same datasets to generate plots using our proposed scaling law in Equation 7 in order to compare them.

Scaling Law	Parameters	Tokens	Sparsities(%)	Test Models
Hoffman [23]	400M–10T	8B–216.2B	–	9
Frantar [24]	1.3M–85M	16B–65B	0, 50, 75, 87.5	48
Abnar [25]	329M–21.2B	15B–128B	0, 25, 50, 75, 90, 95, 98	35

TABLE VI: Parameters, tokens, sparsity, and number of test models collected from the corresponding works.

Along with drawing the plots, we measure the prediction Mean Square Error (MSE) between our proposed scaling law and the respective scaling law for better visualization of prediction of our proposed scaling law.

First, to compare our proposed scaling law in Equation 7 with Hoffman scaling law in Equation 2 [23], we refer back to the Lemma in section III where we have shown that if the sparsity  $S = 0$ , Equation 7 converts into Equation 2. Table VII shows the fitted coefficient values in Equation 7 for the dense models from [23]. Figure 3 shows the loss vs compute budget using the dataset in [23]. On the  $x$ -axis is compute ( $C = 6ND$ ), which depends on model size  $N$  and tokens  $D$  and hence captures the impact of both. On the  $y$ -axis is the calculated loss using both scaling laws. We see an identical plot, indicating that our proposed scaling law behaves the same as the original scaling law for dense models capturing the dense scaling behavior where increasing compute results in decreasing pretraining loss.

Coefficients	$e$	$a$	$b$	$c$	$\alpha$	$\beta$	$\gamma$
Values	1.69	406.4	410.7	0	0.34	0.28	0.01

TABLE VII: Fitted scaling law coefficient values of our proposed scaling law for dense models.

To compare our proposed scaling law with Frantar scaling law, we use the data (sparsity, training steps, number of nonzero parameters and training tokens) collected from the 48 models that were used to conduct the experiments in [24]. Figure 4 shows that our proposed scaling law captures the almost similar scaling behavior as Frantar scaling law for sparse models as sparsity and number of nonzero parameters keep increasing. The loss prediction is very similar with average  $MSE = 0.00078$ . Table VIII shows the fitted parameter values for our proposed scaling law for models from Frantar scaling law experiments [24].

Coefficients	$e$	$a$	$b$	$c$	$\alpha$	$\beta$	$\gamma$
Values	0.15	86.03	7.90	29.26	0.28	0.08	2.00

TABLE VIII: Fitted parameter values of our proposed scaling law for Frantar-style sparse models.

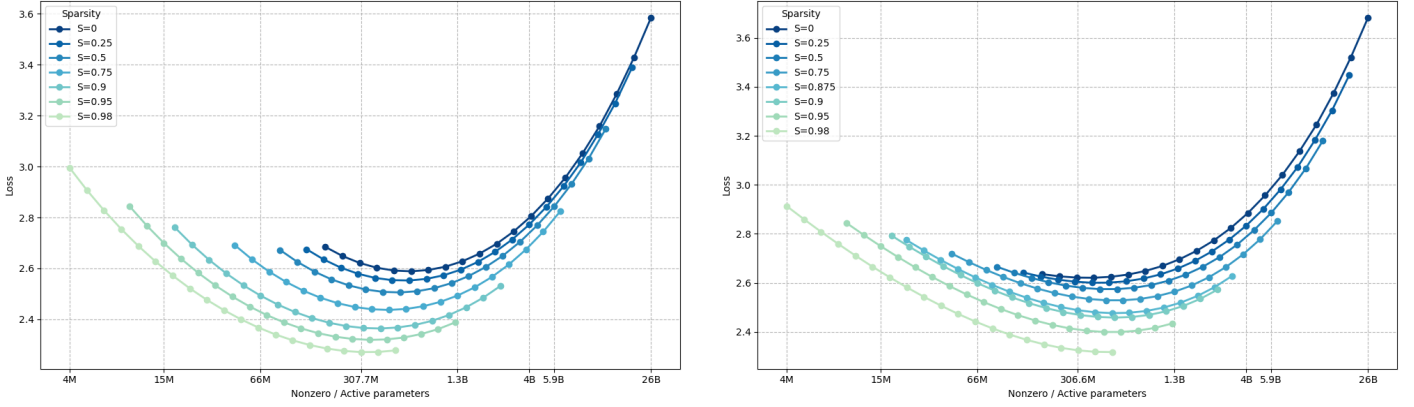


Fig. 6: IsoFLOP plot of Abnar scaling law (left) and our proposed scaling law (right) for a compute budget of  $1e20$  FLOPs.

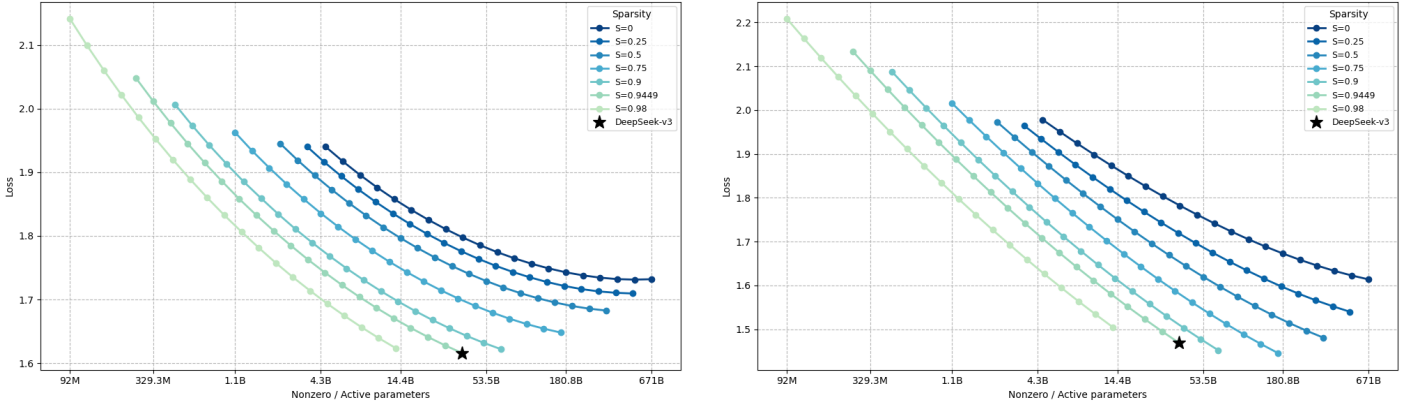


Fig. 7: IsoFLOP plot of Abnar scaling law (left) and our proposed scaling law (right) for a compute budget  $3.29e24$  FLOPs of DeepSeek-V3 training.

We also compared our proposed scaling law with the Abnar scaling law in Equation 5 [25]. For this comparison we use the interpolated values of parameters, tokens, and the exact compute budget of the 35 models used to conduct the experiments in [25]. We have used interpolated values to generate the full dataset because even though the authors have shared a list of compute budget and sparsity levels, no such list was shared for model size and training tokens. So we used the plots shared in [25] and generated the entire dataset. In Figure 5 we have drawn compute budget (FLOPs) vs. loss plots to compare the behavior of both scaling laws. We observe that with the increase of the sparsity and compute, the loss decreases, and both scaling laws show a similar pattern. The average prediction MSE between Abnar scaling law and our proposed scaling law is 0.0005 which is not significant. We present our fitted scaling law coefficient values in Table IX.

Coefficients	$e$	$a$	$b$	$c$	$\alpha$	$\beta$	$\gamma$
Values	0.57	8.26	6324.82	3.57	0.08	0.40	1.19

TABLE IX: Fitted parameter values of our proposed scaling law for MoE-based models.

Abnar et al. [25] also conducted IsoFLOP experiments with the given compute budget of  $1e20$  FLOPs for the MoE-based models. In Figure 6 we have shown the IsoFLOP loss prediction comparison between Abnar scaling law and our proposed scal-

ing law, where each line connects models with different sparsity and model sizes trained under the same amount of compute budget  $1e20$  with active parameters as x-axis and training loss as y-axis. In [25] the authors intentionally cut the plot for active parameters at  $4B$  parameters even though the original experiments had active parameters around  $26B$ . For comparison purpose, we mark that  $4B$  parameter spot and generate the entire plot in Figure 6. For IsoFLOP experiments [25], the authors showed that for fixed sparsity, as we increase number of active parameters, the pretraining loss keeps decreasing until it reaches a sweet spot. Beyond that sweet spot, loss starts increasing again. As seen from Figure 6, our proposed scaling law can effectively capture this behavior.

To demonstrate the effectiveness of our scaling law for larger models, we use DeepSeek-V3 [21] which is a MoE-based model with 671B parameters and 37B of which are activated for each token as an example. The model was trained with  $14.8T$  tokens. Using the compute formula  $C = 6ND$  where  $N$  is the number of active parameters and  $D$  is the number of training tokens, we measure the total compute,  $3.29e24$  used to train DeepSeek-V3. We generate an interpolated IsoFLOP dataset using this compute budget where we restricted the number of total parameters to  $671B$  parameters. Figure 7 shows that our proposed scaling law exhibits a very similar pattern to Abnar scaling law for very large models as well.

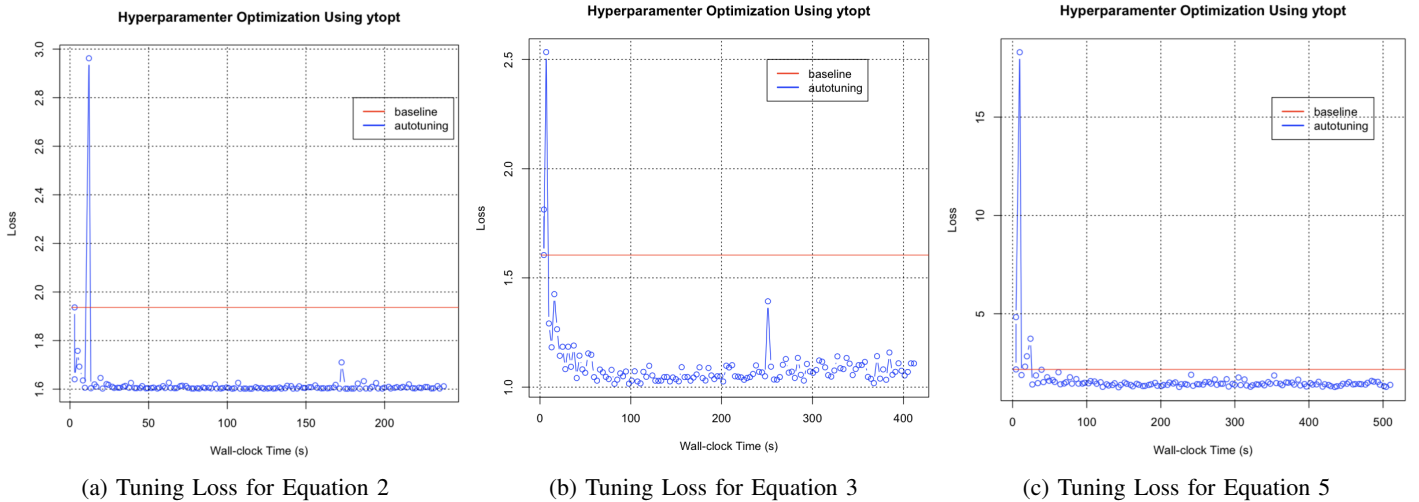


Fig. 8: Loss calculated by the scaling law coefficients generated by ytopt and grid search. The red lines are the loss using the best scaling law coefficients provided in the respective work, and the blue dots are the loss tuned for different evaluations over time using ytopt.

### B. Hyperparameter Optimization for Better Scaling Law Coefficients

Most of the previous scaling laws discussed in this paper used grid search to find the best values for the scaling law coefficients. While grid search is a commonly used approach, it is still inefficient. As an alternative, we have used ytopt [36]–[38] for scaling law coefficient optimization. ytopt is a Bayesian optimization–based autotuner that builds a surrogate model to explore the promising regions to find the optimal values with fewer evaluations. In our previous work [39], ytopt outperformed grid search, random search, a genetic algorithm, and XGBoost in accuracy and tuning time. Unlike traditional autotuners, ytopt leverages libEnsemble’s [40] asynchronous manager-worker framework to run multiple evaluations in parallel, reducing the one-by-one autotuning time.

To use ytopt for the optimization process for finding the best scaling law coefficients for the previous scaling laws, we use the best scaling law coefficients for the scaling laws in Tables II, IV, and V as the baseline and the default values to define the proper search space for each coefficient. We carefully define the range for each coefficient for Equations 2, 3, and 5 and then use ytopt to run the optimization process. The generated hyperparameter optimization results in Figure 8(a), (b), and (c) illustrate that ytopt achieves better loss predictions than grid search. Since ytopt is a Bayesian optimization-based approach, it is much faster than a grid search-based approach and is overall a better alternative.

### C. Discussion

In summary, we observe that our proposed generalized scaling law Equation 7 effectively captures the scaling behavior of Equations 2, 3, and 5 for dense and sparse LLMs. The effectiveness is further justified by the small MSE between the existing scaling law and our proposed scaling law predictions. In Figure 6 and 7 we have seen that our proposed scaling law can capture the IsoFLOP behavior of MoE models as well. So we can conclude that for a given compute budget, our

proposed scaling law can be used to estimate the best model hyperparameters (Model size, Tokens and Compute) for a given sparsity or to identify the optimal sparsity for the given model hyperparameters.

In this work we have generalized the scaling behaviors of dense and sparse models. Our generalized scaling law extends and covers several existing scaling laws. Its limitations are related to the sparsity factor  $c$  and the coefficient  $\gamma$ , which need to be further optimized for larger LLM models.

## V. CONCLUSIONS

As LLMs get larger and more expensive in training, it is crucial for researchers and developers to estimate the expected performance beforehand. Scaling laws thus are critical. While architecture-specific scaling laws give a fine-grained estimation, as more and more new architecture and training methods are being developed, using different scaling laws for each variant becomes impractical. Our generalized scaling law covers densely activated models, pruned models, and MoE models. Empirical results show that our generalized approach can effectively capture the scaling behavior of the architectures.

Because LLMs inference can be memory-bound and compute-intensive, future work will extend the generalized scaling law in training to not only incorporate other scaling laws [30]–[32], [41], [42] but also take into account inference [43], especially recent agentic AI workloads for answering complex questions through reasoning using chain-of-thought prompting. Since the behavior of scaling laws varies based on training and inference approaches, these approaches can be incorporated in the generalized scaling law as well. Unifying different scaling laws into one single representation lays the foundation of architecture-agnostic representation of the scaling behavior of LLMs.

## ACKNOWLEDGMENTS

This work was supported by DOE ASCR SciDAC RAPIDS and OASIS. We acknowledge the Argonne Leadership Computing Facility for use of Polaris under the project EE-ECP. This

material is based upon work supported by the U.S. Department of Energy, Office of Science, under contract number DE-AC02-06CH11357.

## REFERENCES

- [1] A. Vaswani, N. Shazeer, N. Parmar, J. Uszkoreit, L. Jones, A. N. Gomez, L. Kaiser, and I. Polosukhin, "Attention is all you need," *Advances in Neural Information Processing Systems*, vol. 30, 2017.
- [2] J. Devlin, M.-W. Chang, K. Lee, and K. Toutanova, "Bert: Pre-training of deep bidirectional transformers for language understanding," in *Proceedings of the 2019 conference of the North American chapter of the Association for Computational Linguistics: Human Language Technologies, volume 1 (long and short papers)*, 2019, pp. 4171–4186.
- [3] T. Brown, B. Mann, N. Ryder, M. Subbiah, J. D. Kaplan, P. Dhariwal, A. Neelakantan, P. Shyam, G. Sastry, A. Askell *et al.*, "Language models are few-shot learners," *Advances in Neural Information Processing Systems*, vol. 33, pp. 1877–1901, 2020.
- [4] H. Cheng, M. Zhang, and J. Q. Shi, "A survey on deep neural network pruning – taxonomy, comparison," *Analysis, and Recommendations*, 2023.
- [5] N. Shazeer, A. Mirhoseini, K. Maziarz, A. Davis, Q. Le, G. Hinton, and J. Dean, "Outrageously large neural networks: The sparsely-gated mixture-of-experts layer," *arXiv preprint arXiv:1701.06538*, 2017.
- [6] J. W. Rae, S. Borgeaud, T. Cai, K. Millican, J. Hoffmann, F. Song, J. Aslanides, S. Henderson, R. Ring, S. Young *et al.*, "Scaling language models: Methods, analysis & insights from training gopher," *arXiv preprint arXiv:2112.11446*, 2021.
- [7] S. Smith, M. Patwary, B. Norick, P. LeGresley, S. Rajbhandari, J. Casper, Z. Liu, S. Prabhunoy, G. Zerveas, V. Korthikanti *et al.*, "Using DeepSpeed and Megatron to train Tegatron-Turing NLG 530b, a large-scale generative language model," *arXiv preprint arXiv:2201.11990*, 2022.
- [8] R. Thoppilan, D. De Freitas, J. Hall, N. Shazeer, A. Kulshreshtha, H.-T. Cheng, A. Jin, T. Bos, L. Baker, Y. Du *et al.*, "Lamda: Language models for dialog applications," *arXiv preprint arXiv:2201.08239*, 2022.
- [9] A. Chowdhery, S. Narang, J. Devlin, M. Bosma, G. Mishra, A. Roberts, P. Barham, H. W. Chung, C. Sutton, S. Gehrmann *et al.*, "Palm: Scaling language modeling with pathways," *Journal of Machine Learning Research*, vol. 24, no. 240, pp. 1–113, 2023.
- [10] T. OLMo, P. Walsh, L. Soldaini, D. Groeneveld, K. Lo, S. Arora, A. Bhagia, Y. Gu, S. Huang, M. Jordan *et al.*, "2 OLMo 2 Furious," *arXiv preprint arXiv:2501.00656*, 2024.
- [11] R. Child, S. Gray, A. Radford, and I. Sutskever, "Generating long sequences with sparse transformers," *arXiv preprint arXiv:1904.10509*, 2019.
- [12] N. Du, Y. Huang, A. M. Dai, S. Tong, D. Lepikhin, Y. Xu, M. Krikun, Y. Zhou, A. W. Yu, O. Firat *et al.*, "Glam: Efficient scaling of language models with mixture-of-experts," in *International Conference on Machine Learning*. PMLR, 2022, pp. 5547–5569.
- [13] W. Fedus, B. Zoph, and N. Shazeer, "Switch transformers: Scaling to trillion parameter models with simple and efficient sparsity," *Journal of Machine Learning Research*, vol. 23, no. 120, pp. 1–39, 2022.
- [14] B. Zoph, "Designing effective sparse expert models," in *2022 IEEE International Parallel and Distributed Processing Symposium Workshops (IPDPSW)*. IEEE, 2022, pp. 1044–1044.
- [15] N. Muennighoff, L. Soldaini, D. Groeneveld, K. Lo, J. Morrison, S. Min, W. Shi, P. Walsh, O. Tafjord, N. Lambert *et al.*, "Olmoe: Open mixture-of-experts language models," *arXiv preprint arXiv:2409.02060*, 2024.
- [16] A. Liu, B. Feng, B. Wang, B. Wang, B. Liu, C. Zhao, C. Deng, C. Ruan, D. Dai, D. Guo *et al.*, "DeepSeek-v2: A strong, economical, and efficient mixture-of-experts language model," *arXiv preprint arXiv:2405.04434*, 2024.
- [17] D. Dai, C. Deng, C. Zhao, R. Xu, H. Gao, D. Chen, J. Li, W. Zeng, X. Yu, Y. Wu *et al.*, "DeepSeekMoE: towards ultimate expert specialization in mixture-of-experts language models," *arXiv preprint arXiv:2401.06066*, 2024.
- [18] A. Q. Jiang, A. Sablayrolles, A. Roux, A. Mensch, B. Savary, C. Bamford, D. S. Chaplot, D. d. l. Casas, E. B. Hanna, F. Bressand *et al.*, "Mixtral of experts," *arXiv preprint arXiv:2401.04088*, 2024.
- [19] D. Guo, D. Yang, H. Zhang, J. Song, R. Zhang, R. Xu, Q. Zhu, S. Ma, P. Wang, X. Bi *et al.*, "DeepSeek-r1: Incentivizing reasoning capability in LLMs via reinforcement learning," *arXiv preprint arXiv:2501.12948*, 2025.
- [20] A. Radford, J. Wu, R. Child, D. Luan, D. Amodei, I. Sutskever *et al.*, "Language models are unsupervised multitask learners," *OpenAI blog*, vol. 1, no. 8, p. 9, 2019.
- [21] DeepSeek-AI, "DeepSeek-V3 technical report," 2025. [Online]. Available: <https://arxiv.org/abs/2412.19437>
- [22] J. Kaplan, S. McCandlish, T. Henighan, T. B. Brown, B. Chess, R. Child, S. Gray, A. Radford, J. Wu, and D. Amodei, "Scaling laws for neural language models," *arXiv preprint arXiv:2001.08361*, 2020.
- [23] J. Hoffmann, S. Borgeaud, A. Mensch, E. Buchatskaya, T. Cai, E. Rutherford, D. d. L. Casas, L. A. Hendricks, J. Welbl, A. Clark *et al.*, "Training compute-optimal large language models," *arXiv preprint arXiv:2203.15556*, 2022.
- [24] E. Frantar, C. Riquelme, N. Houlsby, D. Alistarh, and U. Evci, "Scaling laws for sparsely-connected foundation models," *arXiv preprint arXiv:2309.08520*, 2023.
- [25] S. Abnar, H. Shah, D. Busbridge, A. M. E. Ali, J. Susskind, and V. Thilak, "Parameters vs flops: Scaling laws for optimal sparsity for mixture-of-experts language models," *arXiv preprint arXiv:2501.12370*, 2025.
- [26] T. Henighan, J. Kaplan, M. Katz, M. Chen, C. Hesse, J. Jackson, H. Jun, T. B. Brown, P. Dhariwal, S. Gray *et al.*, "Scaling laws for autoregressive generative modeling," *arXiv preprint arXiv:2010.14701*, 2020.
- [27] A. Clark, D. de Las Casas, A. Guy, A. Mensch, M. Paganini, J. Hoffmann, B. Damoc, B. Hechtman, T. Cai, S. Borgeaud *et al.*, "Unified scaling laws for routed language models," in *International Conference on Machine Learning*. PMLR, 2022, pp. 4057–4086.
- [28] J. Ludziewski, J. Krajewski, K. Adamczewski, M. Pióro, M. Krutul, S. Antoniak, K. Ciebiera, K. Król, T. Odrzygóźdź, P. Sankowski *et al.*, "Scaling laws for fine-grained mixture of experts," in *Forty-first International Conference on Machine Learning*, 2024.
- [29] S. Y. Gadre, G. Smyrnis, V. Shankar, S. Gururangan, M. Wortsman, R. Shao, J. Mercat, A. Fang, J. Li, S. Keh *et al.*, "Language models scale reliably with over-training and on downstream tasks," *arXiv preprint arXiv:2403.08540*, 2024.
- [30] T. Kumar, Z. Ankner, B. F. Spector, B. Bordelon, N. Muennighoff, M. Paul, C. Pehlevan, C. Ré, and A. Raghunathan, "Scaling laws for precision," *arXiv preprint arXiv:2411.04330*, 2024.
- [31] D. Busbridge, A. Shidani, F. Weers, J. Ramapuram, E. Littwin, and R. Webb, "Distillation scaling laws," 2025. [Online]. Available: <https://arxiv.org/abs/2502.08606>
- [32] M. Chen, C. Zhang, J. Liu, Y. Zeng, Z. Xue, Z. Liu, Y. Li, J. Ma, J. Huang, X. Zhou *et al.*, "Scaling law for quantization-aware training," *arXiv preprint arXiv:2505.14302*, 2025.
- [33] J. Droppo and O. Elibol, "Scaling laws for acoustic models," *arXiv preprint arXiv:2106.09488*, 2021.
- [34] K. Qiu, X. Li, H. Chen, J. Sun, J. Wang, Z. Lin, M. Savvides, and B. Raj, "Efficient autoregressive audio modeling via next-scale prediction," *arXiv preprint arXiv:2408.09027*, 2024.
- [35] A. Aghajanyan, L. Yu, A. Conneau, W.-N. Hsu, K. Hambardzumyan, S. Zhang, S. Roller, N. Goyal, O. Levy, and L. Zettlemoyer, "Scaling laws for generative mixed-modal language models," in *International Conference on Machine Learning*. PMLR, 2023, pp. 265–279.
- [36] X. Wu, P. Balaprakash, M. Kruse, J. Koo, B. Videau, P. Hovland, V. Taylor, B. Geltz, S. Jana, and M. Hall, "ytopt: Autotuning scientific applications for energy efficiency at large scales," *Concurrency and Computation: Practice and Experience*, vol. 37, no. 1, p. e8322, 2025. [Online]. Available: <https://onlinelibrary.wiley.com/doi/abs/10.1002/cpe.8322>
- [37] X. Wu, J. R. Tramm, J. Larson, J.-L. Navarro, P. Balaprakash, B. Videau, M. Kruse, P. Hovland, V. Taylor, and M. Hall, "Integrating ytopt and libEnsemble to autotune OpenMC," *The International Journal of High Performance Computing Applications*, vol. 39, no. 1, pp. 79–103, 2025.
- [38] X. Wu *et al.*, "ytopt: machine-learning-based autotuning and hyperparameter optimization framework using Bayesian Optimization," 2025. [Online]. Available: <https://github.com/ytopt-team/ytopt>
- [39] X. Wu, P. Paramasivam, and V. Taylor, "Autotuning Apache TVM-based scientific applications using Bayesian optimization," in *Proceedings of the SC '23 Workshops of The International Conference on High Performance Computing, Network, Storage, and Analysis*. ser. SC-W '23. New York, NY, USA: Association for Computing Machinery, 2023, pp. 29–35. [Online]. Available: <https://doi.org/10.1145/3624062.3626079>
- [40] S. Hudson, J. Larson, J.-L. Navarro, and S. M. Wild, "libEnsemble: A library to coordinate the concurrent evaluation of dynamic ensembles of calculations," *IEEE Transactions on Parallel and Distributed Systems*, vol. 33, no. 4, pp. 977–988, 2021.
- [41] H. Wang, S. Ma, R. Wang, and F. Wei, "Q-sparse: All large language models can be fully sparsely-activated," *arXiv preprint arXiv:2407.10969*, 2024.
- [42] V. Thangarasa, A. Gupta, W. Marshall, T. Li, K. Leong, D. DeCoste, S. Lie, and S. Saxena, "SPDF: Sparse pre-training and dense fine-tuning for large language models," in *Uncertainty in Artificial Intelligence*. PMLR, 2023, pp. 2134–2146.
- [43] N. Sardana, J. Portes, S. Doubov, and J. Frankle, "Beyond Chinchilla-Optimal: Accounting for inference in language model scaling laws," 2025. [Online]. Available: <https://arxiv.org/abs/2401.00448>